Astronomy & Astrophysics

L<small>ETTER TO THE</small> E<small>DITOR</small>

A closer look at supernovae as seeds for galactic magnetization

Evangelia Ntormousi[1,2], Fabio Del Sordo[3,4,5], Matteo Cantiello[6], and Andrea Ferrara[1]

[1] Scuola Normale Superiore, Piazza dei Cavalieri, 7, 56126 Pisa, Italy
e-mail: `entorm@physics.uoc.gr`
[2] Institute of Astrophysics, Foundation for Research and Technology (FORTH), Nikolaou Plastira 100, Vassilika Vouton, 711 10 Heraklion, Crete, Greece
[3] Institute of Space Sciences (ICE-CSIC), Campus UAB, Carrer de Can Magrans s/n, 08193 Barcelona, Spain
[4] Institut d'Estudis Espacials de Catalunya (IEEC), Carrer del Gran Capità 2, 08034 Barcelona, Spain
[5] INAF, Osservatorio Astrofisico di Catania, Via Santa Sofia, 78, Catania, Italy
[6] Center for Computational Astrophysics, Flatiron Institute, 62 5th Ave, New York, NY 10010, USA

ABSTRACT

Context. Explaining the currently observed magnetic fields in galaxies requires relatively strong seeding in the early Universe. One of the current theories proposes that magnetic seeds on the order of μG were expelled by supernova (SN) explosions after primordial fields of nG strength or weaker were amplified in stellar interiors.

Aims. In this work, we take a closer look at this theory and calculate the maximum magnetic energy that can be injected in the interstellar medium by a stellar cluster of mass M_{cl} based on what is currently known about stellar magnetism.

Methods. We consider early-type stars and adopt either a Salpeter or a top-heavy initial mass function. For their magnetic fields, we adopt either a Gaussian or a bimodal distribution. The Gaussian model assumes that all massive stars are magnetized with $10^3 < \langle B_* \rangle < 10^4$ G, while the bimodal, consistent with observations of Milky Way stars, assumes only $5-10\%$ of OB stars have $10^3 < \langle B_* \rangle < 10^4$ G, while the rest have $10 < \langle B_* \rangle < 10^2$ G. We ignore the effect of magnetic diffusion and assume no losses of magnetic energy.

Results. We find that the maximum magnetic energy that can be injected by a stellar population is between 10^{-10} and 10^{-7} times the total SN energy. The highest end of these estimates is about five orders of magnitude lower than what is usually employed in cosmological simulations, where about 10^{-2} of the SN energy is injected as magnetic.

Conclusions. Pure advection of the stellar magnetic field by SN explosions is a good candidate for seeding a dynamo, but not enough to magnetize galaxies. Assuming SNe as the main mechanism for galactic magnetization, the magnetic field cannot exceed an intensity of 10^{-7} G in the best-case scenario for a population of 10^5 solar masses in a superbubble of 300 pc radius, while more typical values are between 10^{-10} and 10^{-9} G. Therefore, other scenarios for galactic magnetization at high redshift need to be explored.

Key words. magnetic fields – stars: magnetic field – ISM: magnetic fields – galaxies: magnetic fields

1. Introduction

The origin of magnetic fields is one of the most compelling problems in astrophysics and cosmology. While some constraints of the primordial magnetic field strength exist, the mechanism that can generate them are very diverse (e.g., Gnedin et al. 2000; Subramanian 2019). What we do know is that the magnetic fields currently observed in spiral galaxies are too strong to be primordial. Therefore, they were either seeded by a primordial field in the early Universe and then amplified through a dynamo, or directly generated by an astrophysical process in galaxies (e.g., Brandenburg & Ntormousi 2022).

One theory for magnetizing early galaxies involves stars (Rees 1987). The idea is that a dynamo process in stellar interiors amplifies the tiny magnetic seeds coming from a Biermann battery or similar mechanism. When these stars explode as supernovae (SNe), the amplified fields are injected in the surrounding interstellar medium (ISM).

A number of numerical experiments adopt this mechanism as a subgrid model in galactic dynamo (Hanasz et al. 2009; Kulpa-Dybeł et al. 2011, 2015; Butsky et al. 2017) or cosmological structure formation simulations (Beck et al. 2013,

Vazza et al. 2017; Katz et al. 2019; Garaldi et al. 2021; Martin-Alvarez et al. 2021), injecting a magnetic field together with thermal and kinetic energy as feedback from stellar populations. However, the assumptions about the relative ratio of magnetic to thermal SN energy differ strongly between models. For instance, Kulpa-Dybeł et al. (2011, 2015) assume that 10% of the SNe introduce a field on the order of 10^{-5} μG in dense regions of the ISM. A similar assumption on the incidence of SN magnetization is made by Hanasz et al. (2009); although, they do not specify the value of the magnetic field. Butsky et al. (2017) seed each SN event with 10^{-7} of the SN energy as magnetic energy. Cosmological models typically assume that the contribution from SN is much larger, and inject an energy $E_{mag,inj} = \epsilon E_{SN}$ with ϵ typically ranging from 0.01 to 0.03. This implies field strengths of about 10^{-4} G on the typical scale of a remnant, which is about $5-10$ pc. While these approaches provide a useful starting point for structure formation and cosmological simulations, they are not based on detailed models or observations of stellar magnetism.

In this Letter, we use our current understanding of stellar magnetism to provide a simple estimate of the maximum amount of magnetic energy that can be injected by a primordial

stellar population. To our knowledge, this estimate has not been performed previously, and it can be very useful for studies of cosmological magnetic field evolution. We show that the typical magnetic seeding by SN explosions used so far in cosmological simulations is much larger than what can be produced by a typical stellar population. Instead, the smaller values assumed by some galactic dynamo models are closer to our estimates.

2. Stellar magnetic fields

Equipartition between magnetic energy and gravitational binding energy sets the maximum-allowed magnetic field $B_{max} \propto M/R^2$ in a star. In early-type stars, this maximum surface magnetic field is about 10^7 G. On the other hand, the largest observed fields at the surface of stars seem to be much smaller, with $B_{max,obs} \sim \left(10^{-3}-10^{-4}\right) B_{max}$ (Braithwaite & Spruit 2017). This means that magnetic fields usually provide a very small perturbation to the stellar hydrostatic equilibrium. Also, in early-type stars, the maximum observed amplitude of surface magnetic fields is 10^3-10^4 G (Petit et al. 2019).

The origin and evolution of stellar magnetism is not fully understood. It is clear that dynamo action can amplify a seed magnetic field in stars, with the dynamo tapping into the energy reservoir provided by turbulent convection and/or differential rotation (Brandenburg et al. 2012). This is the case of the Sun and of low-mass stars in general. On the other hand, the large-scale, high amplitude fields observed at the surface of 5−10% of early-type stars ("fossil fields") are thought to be inherited during the star formation process (e.g., Donati & Landstreet 2009). It is also possible that some of these fields are created via interactions with a companion star (Ferrario et al. 2009). Finally, dynamo action might be at play in the interiors of early-type stars as well, in their convective cores (Augustson et al. 2016), near-surface convective zones (Cantiello & Braithwaite 2011), and radiative regions (Spruit 2002; Wheeler et al. 2015; Fuller et al. 2019).

As we outlined in the introduction, state-of-the-art cosmological models and some galactic dynamo models approach stellar magnetic seeding by introducing a magnetic field corresponding to roughly 1% the SN energy in feedback regions. The motivation behind this choice is based on estimates from galactic SN remnants. For instance, Beck et al. (2013) estimate an average SN remnant with a radius of 5 pc and magnetic field strength 10^{-4} G, citing the review of magnetism around local SN remnants by Reynolds et al. (2012). This estimate corresponds to about 6×10^{48} erg in total magnetic energy. However, assuming that such strong magnetic fields at the SN stage come directly from the progenitor implies paradoxically high magnetization for the star. If the interstellar medium at the typical radius of a SN remnant R_{SN} contains $E_{mag,inj} = 0.01 E_{SN}$, with $E_{SN} = 10^{51}$ erg, then the magnetic energy density of the progenitor would be $E_{mag,inj}$ divided by the volume of the star:

$$u_{mag,*} = E_{mag,inj}/V_*, \qquad (1)$$

assuming no magnetic energy was lost or gained during the explosion. For an O-type star with a radius $R_* = 100 R_\odot$ and $E_{mag,inj} = 10^{49}$ erg, $u_{mag,*} \simeq 10^{10}$ erg cm^{-3}. Since $u_{mag} = B^2/8\pi$, the typical magnetic field of the progenitor would be roughly $B_* = 10^5-10^6$ G. This number is at least one order of magnitude larger than the maximum magnetic field observed at the surface of early-type stars (e.g., Petit et al. 2019). This inconsistency is exacerbated assuming a smaller radius for the progenitor star, or dissipative losses during the evolution of the SN.

Clearly, the typical values for SN-injected magnetic fields used so far in cosmological simulations are unreasonably high; although, they match the observed magnetic fields around local SN remnants, which are on the order of a few microgauss to a milligauss. However, there is currently no theory that involves magnetization of the SN ejecta to explain these values. Instead, current theories involve the amplification of the magnetic field surrounding the remnant, through either compression and turbulence (Inoue et al. 2009), or a cosmic-ray-driven dynamo (e.g., Xu & Lazarian 2017). In the following section, we attempt to make a physically meaningful estimate for magnetic seeding from SNe.

3. The maximum SN-injected magnetic energy from a stellar population

We construct a simple model for the magnetization of a primordial cloud by SN ejecta. In this model, we assume that the stars return all of their magnetic field to the ISM. In doing so, we implicitly require that the entire mass of the star is ejected in the ISM, neglecting the mass and magnetization of the resulting compact object. Obviously, this assumption is not true for most massive stars, but it helps our purpose of calculating an upper limit to the magnetic field that can be injected by the population. We also neglect dissipative losses or other forms of magnetic energy gain, so that the magnetic energy is conserved.

The model essentially consists of the following relation for the total magnetic energy generated by a cluster of mass M_{cl}:

$$E_{mag,cl} = \int_{M_{SN}}^{M_{max}(M_{cl})} \xi(m) \left(\frac{B_*^2}{8\pi}\right) \left(\frac{4\pi R_*(m)^3}{3}\right) dm, \qquad (2)$$

where $\xi(m)$ is the assumed initial mass function (IMF) of the primordial stellar population, B_* the magnetic field of a star of mass m[1], $R_*(m)$ its radius, M_{SN} the minimum mass for SNe, and $M_{max}(M_{cl})$ the maximum stellar mass of a cluster of mass M_{cl}. We subsequently estimate $E_{mag,cl}$ for different masses of the stellar cluster. All the quantities that enter Eq. (2) are only partially known, with $\xi(m)$ and B_* being the least understood so far. However, we can make order-of-magnitude estimates based on what is currently known.

3.1. IMF of the star cluster

The IMF of stars in primordial, low-metallicity environments is highly uncertain. Numerical work (e.g., Clark et al. 2008; Dopcke et al. 2013; Chon et al. 2021) has shown that for metallicities below $Z/Z_\odot \simeq 10^{-5}$, fragmentation becomes inefficient and the stellar IMF favors high-mass stars, with an almost flat distribution at high masses. Above this metallicity limit, simulations recover a Salpeter-like power-law slope in high masses (Salpeter 1955). Therefore, here we use two IMF models: (i) a Salpeter IMF, $\xi_S(m) = \xi_0 m^{-2.35}$ (which for $m > 0.5 M_\odot$ coincides with the Kroupa 2001 and Chabrier 2003 models); and (ii) a top-heavy IMF, with a high-mass slope of -1.5: $\xi_{TH}(m) = \xi_0 m^{-1.5}$. As limits in the integration of the IMF, we set $M_{SN} = 8 M_\odot$ and $M_{max}(M_{cl}) = 1.2 \cdot M_{cl}^{0.45}$ (Larson 2003). Finally, for $R_*(m)$, we use the simple relation for nonconvective stars, $R_*(m) \propto m^{0.57}$.

---

[1] B_* does not depend on m in this model, in agreement with the existing observations of massive stars (Wade & MiMeS Collaboration 2015).
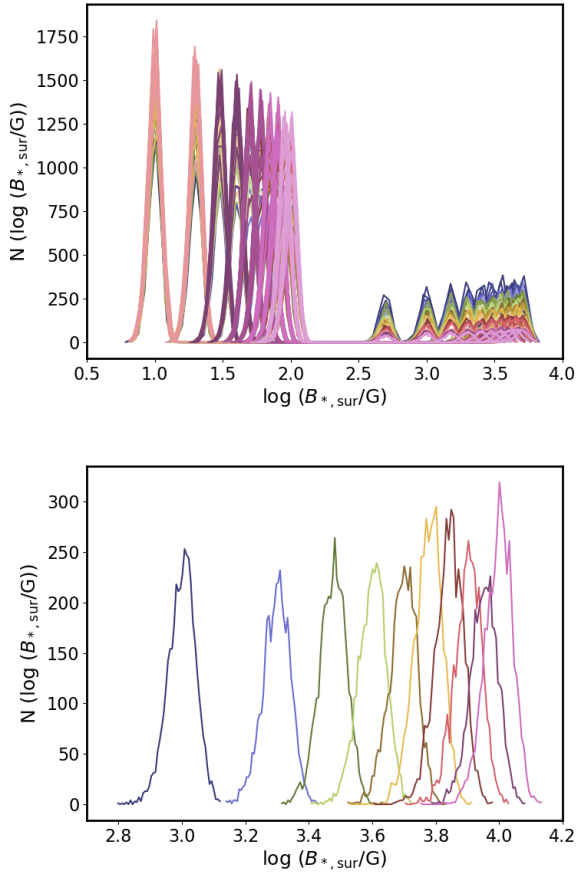
Fig. 1. Range of stellar surface stellar magnetic field distributions used in the two models. *Top:* bimodal distribution model. *Bottom:* single Gaussian model. Both models are shown here for a cluster of $10^5 \, M_\odot$ and a Salpeter IMF. Each color corresponds to a set of parameters for each distribution: (μ_1, μ_2, f_2) for the bimodal, and μ for the Gaussian. The dispersion of each distribution with mean μ_i is set to $\sigma_i = 0.1\mu_i$.

3.2. Stellar magnetic field distribution

For the distribution of B_* we use two different models, starting from assumptions about the surface magnetic field of the stars. The first model is driven from local observations of early-type stars, which show a very low incidence of detectable magnetization. Specifically, only about 5 to 10% of the observed stars host magnetic fields of $10^3 - 10^4$ G, while the rest fall below about 100 G (Hubrig et al. 2011; Alecian et al. 2014; Morel et al. 2014; Wade et al. 2014; Petit et al. 2019). In fact, there are indications that OB stars present a magnetic dichotomy similar to that observed for Ap stars. Interestingly, the incidence of high magnetization does not seem to correlate with the stellar parameters (Wade & MiMeS Collaboration 2015). Therefore, our first model approximates the distribution of stellar surface magnetic fields, $B_{*,\mathrm{sur}}$, as a bimodal for all the stars contained in the integral of Eq. (2). The parameters of the distribution are the two means, μ_1 and μ_2, which we vary from $10 \, \mathrm{G} < \mu_1 < 100 \, \mathrm{G}$ and $500 \, \mathrm{G} < \mu_2 < 5 \times 10^3 \, \mathrm{G}$, respectively, and f_2, the incidence of highly magnetized stars, which takes values from $0.05 < f_2 < 0.2$.

Recently, Farrell et al. (2022) showed that the surface magnetic field distribution of AB stars is well fitted by a Gaussian with a mean at about 1 kG. Although their study involved less massive stars, we explore a second model where all OB stars are strongly magnetized, in order to push our calculations toward an

upper limit. In this case, $B_{*,\mathrm{sur}}$ is a single Gaussian with a peak that we vary between $10^3 < \mu < 10^4$ G. The two panels of Fig. 1 illustrate the resulting range of B_* distributions for the two models, for a stellar population of $10^5 \, M_\odot$. The different line colors correspond to different sets of parameters.

Going from the surface to the global field strength requires an assumption as to the internal magnetic field distribution. Here, we assume a dipole distribution of the magnetic field strength as a function of radius r:

$$B*(r) = \int_{R_{\mathrm{core}}}^{R_*} 4\pi r^2 B_{*,\mathrm{sur}} \left(\frac{R_*}{r}\right)^3 \mathrm{d}r. \tag{3}$$

Since the dipole field diverges at the center, in Eq. (3) the integration starts from a core radius, R_{core}. O- and B-type stars rotate rapidly and possess convective cores, which means that a dynamo could act in their interior (Augustson et al. 2016). Although a core dynamo cannot be an explanation for the strong surface fields (since there is no time for such a field to reach the surface – Charbonneau & MacGregor 2001), a fossil field from a convective core could still be partly expelled with the SN. Equipartition fields in the convective cores of OB stars are expected to be in the range $10^5 - 10^6$ G (Augustson et al. 2016). With this in mind, we estimate R_{core} as the largest of two radii: (i) the radius at which the magnetic field strength from Eq. (3) reaches the maximum stable field according to dynamo models (e.g., Augustson et al. 2016), $B_*(R_{\mathrm{core}}) = 10^6$ G; or (ii) the mean core radius for massive stars, $R_{\mathrm{core}} = 0.2 \, R_*$[2]. Inside the core, the magnetic field is considered constant, either at the maximum value of 10^6 G or to the value reached at R_{core} from Eq. (3).

3.3. Results

Figure 2 shows the result of this calculation in terms of the fraction of injected magnetic energy $E_{\mathrm{mag,inj}}$ over total SN energy $E_{\mathrm{SN,tot}}$. This quantity is equivalent to the factor ϵ employed in numerical simulations of magnetic field injection. Even at the highest limit of this range, assuming a top-heavy IMF and all the stars strongly magnetized (red line of the bottom panel), ϵ does not exceed 10^{-7}. This strong upper limit value is still 10^5 times lower than the number typically assumed in cosmological models.

Figure 3 shows the same results in terms of the magnetic field strength. Here, we have carried out two calculations, corresponding to two approaches of distributing the SN ejecta. One assumes that all the stars deposit their magnetic energy in a single superbubble with a radius of 300 pc (so that their magnetic energies are added), and this is shown as solid lines. The other, shown in dashed lines, assumes that each star explodes in isolation, forming a SN remnant with an average radius of 30 pc (so that their magnetic energies are averaged). In reality, both scenarios are possible, depending on the clustering of the stars. Here, we see that an extremely massive cluster, with a top-heavy IMF and all of its early-type, strongly magnetized stars, depositing their magnetic field in a single superbubble of just a 300 pc radius, would yield a magnetic field of about 10^{-7} G. More typical values instead are between $10^{-10} - 10^{-8}$ G, which is comparable to other primordial seeding mechanisms.

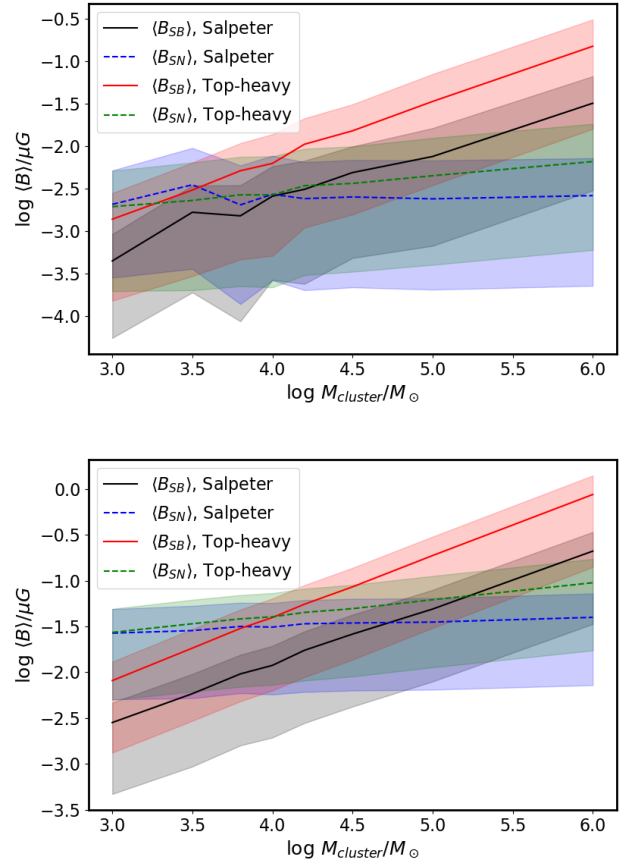[2] Varying the range of $R_{\mathrm{core}} = 0.2 - 0.4 \, R_*$ has a negligible effect on the results.
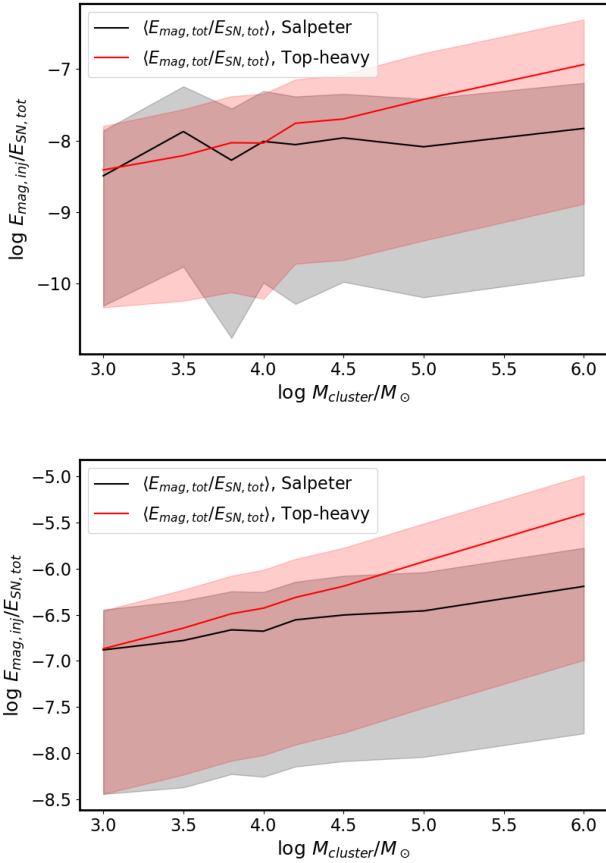
Fig. 2. Magnetic energy injected by a stellar population of mass $M_{\rm cluster}$ over SN energy of the same population. The latter is calculated as 10^{51} erg times the total number of massive stars. The shaded area shows the range of values assuming different magnetic field distributions for the stars. The *top panel* assumes bimodal magnetic field distributions (top panel of Fig. 1) and the *bottom* one assumed Gaussian ones (bottom panel of Fig. 1). The two lines in each panel show results for different IMFs.

Fig. 3. Total magnetic field in a single superbubble, $\langle B_{\rm SB} \rangle$, or mean magnetic field in SN remnants, $\langle B_{\rm SN} \rangle$, injected by a stellar population of mass $M_{\rm cluster}$. The *top panel* assumes bimodal magnetic field distributions (top panel of Fig. 1) and the *bottom* one assumes Gaussian ones (bottom panel of Fig. 1). Results are shown for different IMFs, with the shaded areas indicating the range over different stellar magnetic field distributions.

4. Discussion

We have shown that the magnetic fields used in cosmological simulations (e.g., Beck et al. 2013; Vazza et al. 2017; Katz et al. 2019; Garaldi et al. 2021; Martin-Alvarez et al. 2021) under the SN-injection scenario are exceedingly high. However, in cosmic-ray-driven galactic dynamo simulations, Hanasz et al. (2009) and Kulpa-Dybeł et al. (2011, 2015) only introduced magnetization in 10% of the SN events. This approach could be considered equivalent to our bimodal distribution of stellar magnetization, with the employed values (10^{-5} µG) lower than our average estimates. Butsky et al. (2017) used magnetic seeds with strengths close to those we predict in this Letter: they injected about 6×10^{-7} of the total SN energy as magnetic energy. All the above works found these small values to be sufficient for driving a galactic dynamo.

The upper limits we calculate here are sensitive to the assumed magnetic field distribution in the stellar interior and to the maximum-allowed surface magnetic field strengths. Assuming a constant magnetic field, $B_* = B_{\rm sur}$, in the entire volume of the star instead of a truncated dipole lowers our estimates for the magnetic energy injection by roughly an order of magnitude. Allowing for extreme surface magnetic fields on the order of a few times 10^5 G increases the maximum magnetic yield by roughly a factor of 200.

We note that our model does not take any dissipative process into account. Moreover, we do not consider the magnetization of the compact objects left behind by the SNe: they could retain a significant amount of the magnetic energy assumed to be injected into the ISM.

Finally, here we have examined the effect of the short-lived, explosive, early-type stars on magnetic field seeding. However, stellar magnetic field injection is also possible through a dynamo-active accretion disk around a protostar. These dynamo-generated fields are strong enough to launch a wind, which in turn could magnetize the ISM (e.g., Brandenburg 2000; von Rekowski et al. 2003; Dyda et al. 2018). Such disks are long-lived for low-mass stars, which can keep seeding the ISM with low levels of magnetization on small scales. This scenario is worth investigating with dedicated numerical models.

5. Conclusions

We conclude that stellar magnetic fields purely advected through SN explosions can tap only 10^{-10}–10^{-7} of the SN explosion energy. The highest limit of these estimates is five orders of magnitude lower than what is currently used in cosmological simulations, even without accounting for diffusion or a residual magnetization of the compact object. Therefore, SN-injected magnetic fields can only provide the seed for additional

processes, such as a turbulent dynamo, which can amplify them to the near-equipartition values measured in local galaxies. Since early galaxies do host strong turbulence, this scenario can be probed with high-resolution simulations of these systems. The obvious next step for this investigation involves resolved numerical simulations of SN-injected fields that can account for magnetic diffusion and model possible dynamo action.

References

Alecian, E., Kochukhov, O., Petit, V., et al. 2014, A&A, 567, A28
Augustson, K. C., Brun, A. S., & Toomre, J. 2016, ApJ, 829, 92
Beck, A. M., Dolag, K., Lesch, H., & Kronberg, P. P. 2013, MNRAS, 435, 3575
Braithwaite, J., & Spruit, H. C. 2017, R. Soc. Open Sci., 4, 160271
Brandenburg, A. 2000, Philos. Trans. R. Soc. London A, 358, 759
Brandenburg, A., & Ntormousi, E. 2022, ArXiv e-prints [arXiv:2211.03476]
Brandenburg, A., Sokoloff, D., & Subramanian, K. 2012, Space Sci. Rev., 169, 123
Butsky, I., Zrake, J., Kim, J.-H., Yang, H.-I., & Abel, T. 2017, ApJ, 843, 113
Cantiello, M., & Braithwaite, J. 2011, A&A, 534, A140
Chabrier, G. 2003, PASP, 115, 763
Charbonneau, P., & MacGregor, K. B. 2001, ApJ, 559, 1094
Chon, S., Omukai, K., & Schneider, R. 2021, MNRAS, 508, 4175
Clark, P. C., Glover, S. C. O., & Klessen, R. S. 2008, ApJ, 672, 757
Donati, J. F., & Landstreet, J. D. 2009, ARA&A, 47, 333
Dopcke, G., Glover, S. C. O., Clark, P. C., & Klessen, R. S. 2013, ApJ, 766, 103
Dyda, S., Lovelace, R. V. E., Ustyugova, G. V., Koldoba, A. V., & Wasserman, I. 2018, MNRAS, 477, 127
Farrell, E., Jermyn, A. S., Cantiello, M., & Foreman-Mackey, D. 2022, ApJ, 938, 10
Ferrario, L., Pringle, J. E., Tout, C. A., & Wickramasinghe, D. T. 2009, MNRAS, 400, L71
Fuller, J., Piro, A. L., & Jermyn, A. S. 2019, MNRAS, 485, 3661
Garaldi, E., Pakmor, R., & Springel, V. 2021, MNRAS, 502, 5726
Gnedin, N. Y., Ferrara, A., & Zweibel, E. G. 2000, ApJ, 539, 505
Hanasz, M., Wóltański, D., & Kowalik, K. 2009, ApJ, 706, L155
Hubrig, S., Schöller, M., Kharchenko, N. V., et al. 2011, A&A, 528, A151
Inoue, T., Yamazaki, R., & Inutsuka, S.-I. 2009, ApJ, 695, 825
Katz, H., Martin-Alvarez, S., Devriendt, J., Slyz, A., & Kimm, T. 2019, MNRAS, 484, 2620
Kroupa, P. 2001, MNRAS, 322, 231
Kulpa-Dybeł, K., Otmianowska-Mazur, K., Kulesza-Żydzik, B., et al. 2011, ApJ, 733, L18
Kulpa-Dybeł, K., Nowak, N., Otmianowska-Mazur, K., et al. 2015, A&A, 575, A93
Larson, R. B. 2003, in Galactic Star Formation Across the Stellar Mass Spectrum, eds. J. M. De Buizer, & N. S. van der Bliek, ASP Conf. Ser., 287, 65
Martin-Alvarez, S., Katz, H., Sijacki, D., Devriendt, J., & Slyz, A. 2021, MNRAS, 504, 2517
Morel, T., Castro, N., Fossati, L., et al. 2014, The Messenger, 157, 27
Petit, V., Wade, G. A., Schneider, F. R. N., et al. 2019, MNRAS, 489, 5669
Rees, M. J. 1987, Q. J. R. Astron. Soc., 28, 197
Reynolds, S. P., Gaensler, B. M., & Bocchino, F. 2012, Space Sci. Rev., 166, 231
Salpeter, E. E. 1955, ApJ, 121, 161
Spruit, H. C. 2002, A&A, 381, 923
Subramanian, K. 2019, Galaxies, 7, 47
Vazza, F., Brüggen, M., Gheller, C., et al. 2017, Class. Quant. Grav., 34, 234001
von Rekowski, B., Brandenburg, A., Dobler, W., Dobler, W., & Shukurov, A. 2003, A&A, 398, 825
Wade, G. A., & MiMeS Collaboration 2015, in Physics and Evolution of Magnetic and Related Stars, eds. Y. Y. Balega, I. I. Romanyuk, & D. O. Kudryavtsev, ASP Conf. Ser., 494, 30
Wade, G. A., Grunhut, J., Alecian, E., et al. 2014, in Magnetic Fields throughout Stellar Evolution, eds. P. Petit, M. Jardine, & H. C. Spruit, 302, 265
Wheeler, J. C., Kagan, D., & Chatzopoulos, E. 2015, ApJ, 799, 85
Xu, S., & Lazarian, A. 2017, ApJ, 850, 126